View metadata, citation and similar papers at core.ac.uk
brought to you by CORE
provided by UPCommons. Portal del coneixement obert de la UPC

ELECTROMAGNETIC EMISSION ANALYSIS OF A MULTIBAND EMI FILTER BASED ON SUB-WAVELENGTH RESONATORS

J.M. Ruiz[1], I. Gil[2] and M. Morata[1]
[1]Escuela Universitaria Salesiana de Sarriá, Psg. Sant Joan Bosco 74, Barcelona, E-08017 Spain.
[2]Department of Electronics Engineering, UPC Barcelona Tech, Colom 1, Terrassa, E-08222 Spain.

A**bstract**: In this paper the electromagnetic emission of sub-wavelength EMI filter based on SRR and CSRR resonator has been analysed by means of near E and H fields simulation with the FDTD SEMCAD® software. The target bands are 900MHz (RFID UHF), 1.8GHz (GSM) and 2.4GHz (ISM, Instrumentation, Scientific and Medical). A 3-stages/5-stages rejection band filter was designed and fabricated in a PCB. The preliminary simulation results show that the more significant emissions take place at higher frequencies, the 1.8 GHz GSM band and ISM band (2.4 GHz), and are located at the resonators' surface.

Keywords: EMI filters, Electromagnetic Compatibility, split ring resonators (SRRs), complementary spiral resonators (CSRs).

1. INTRODUCTION

The increasing of the electromagnetic emissions in the last years requires the design of electronic systems which are immune to electromagnetic interferences (EMI). These new electronic systems must also fulfill the international regulations requirements for radiated emissions, in order to ensure the compatibility with other electronic devices. Since low cost and highly-integrated circuits and systems are required, new filtering techniques are necessary to reduce cost and dimensions of standard EMI filters. In this direction, new solutions have been developed based on Electromagnetic Band Gaps [1][2], a type of metamaterials. Metamaterials are artificial fabricated materials based on periodic o quasi–periodic structures with electromagnetic controllable properties. Among them, we can find the sub-wavelength resonators named split-ring resonator (SRR) [3] and the complementary split-ring resonator (CSRR) [4,5], which are used to reduce the EMI in printed circuit boards (PCB).

In this paper, the electromagnetic emissions of a multiband microstrip filter based on SRRs and CSRRs have been analyzed. The filter has been designed for the target frequency bands of RFID UHF, GSM and the 2.4 GHz industrial, scientific and medical (ISM) band. The electromagnetic radiated emissions have been evaluated by means of the commercial SEMCAD software [6]. Moreover, the insertion losses (S21) and return losses (S11) have been experimentally measured.

The paper is organized as follows: Section 2 is about the circuit design, Section 3 shows the experimental and simulated results and Section 4 summarizes the conclusions.

2. EMI FILTER DESIGN

A complete discussion for the design and preliminary results can be found at [5] and [7]. The starting point consists of a conventional microstrip line which can be potentially affected by RFI in the range of RFID UHF (f_{o1}~900MHz), GSM frequency uplink and downlink bands (f_{o2}~1.8GHz) and ISM (f_{o3}~2.45GHz).

The sub-wavelength particles considered in this work correspond to the original SRR and the dual counterpart of the SR, the CSR. Fig. 1 shows the implemented layout of the EMI filter. The design strategy is based on the implementation of the SRRs in order to develop the stop-band filter at the higher frequency band (ISM). These particles have been etched in the top side of the PCB, close to the host microstrip line. Specifically, a 5-stage SRR has been implemented (Fig. 2(a)) for the ISM band. Concerning the lower frequency bands (i.e. the corresponding with the higher dimensions required resonators), two arrays of 3-stage CSRs have been used in order to develop the stop-band responses at RFID UHF and GSM. They can be etched in the metal ground plane of the PCB and, therefore, no extra area is required (Fig. 2(d)).

The EMI filter was fabricated by using a *Rogers RO3010* substrate (dielectric permittivity, ε_r=10.2 and thickness, h=1.27mm). A 50Ω microstrip line, with 1.18mm width and 47mm length was inserted. A square topology has been chosen for all the resonators in order to enhance the coupling to the host line. Since the distance of the SRRs to the host line is a key point, they have been placed as close as possible to the microstrip line (200µm). Concerning CSRs, they have been etched underneath the microstrip line in order to maximize the electrical coupling to it. Because the number of resonators stages determines the level of rejection of each stop-band filter response, a higher rejection level is expected in case of SRRs. The reduction in the number of stages of CSRs is due to the requirement to include two rejection bands. Finally, the distance between adjacent SRRs and CSRs has a direct impact in the rejection bandwidth. Therefore, it has been also considered as a significant parameter for the final implementation (200µm).

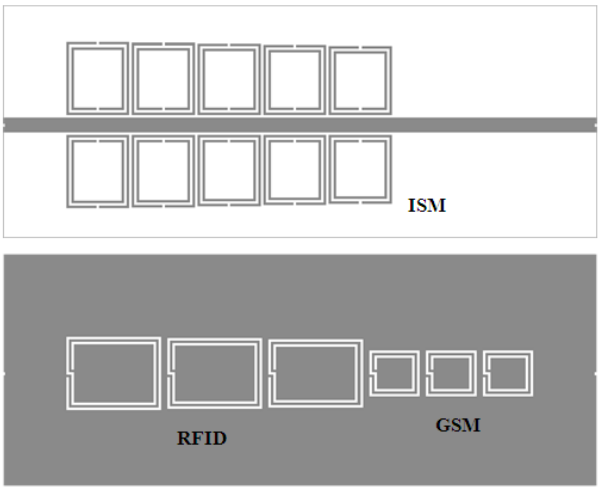

Figure 1. Topology of the designed multiband microstrip EMI filter. (a) Top layer with microstrip line and the SRRs designed at 2.45GHz. (b) Bottom layer with CSRs etched in the ground metal tuned at 900MHz and 1.8GHz, respectively. Metallization zones are depicted in grey.

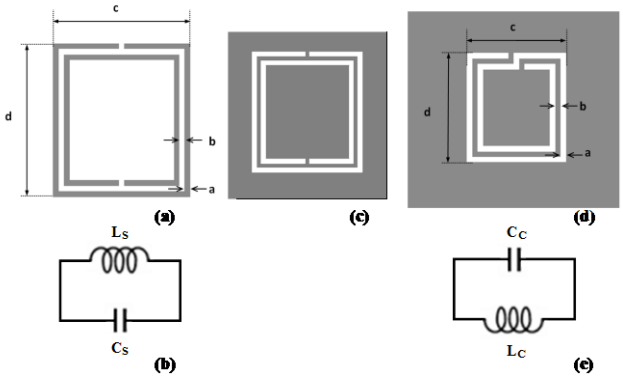

Figure 2. Sub-wavelength particles dimensions: a = b = 0.2mm for all the particles. ISM: c = 5mm, d = 5.5-5.8mm. GSM: c = 3.7mm, d = 4mm. RFID: c= 5.5-5.9mm, d = 7.5mm.

3. RESULTS

A. Measured S11 and S21 parameters.

Fig. 3 shows the measured results of insertion losses (S21) and return losses (S11) [7]. Concerning the rejection level, a higher level is achieved at the ISM band by means of the SRRs, due to the larger number of implemented stages. This fact also implies a wider bandwidth in the stop-band frequency response. The losses of the allowed bands present an average value of 1.5 dB and are basically due to the presence of connectors and ohmic losses. Measured return losses show a low level at the allowed frequency bands (less than 10 dB).

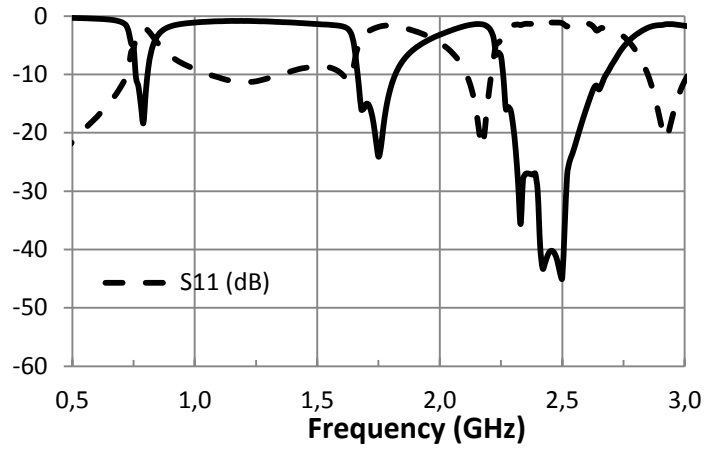

Figure 3. Experimentally measured frequency responses of the insertion losses (S21) and return losses (S11).

B. Simulated Radiation pattern.

The electromagnetic emissions simulation have been performed by using the Finite-Difference Time Domain (FDTD) *SEMCAD software*. To determine the most relevant radiation frequencies, an analysis of the previous results should be done. These frequencies correspond to those that have a higher value of the total power losses, obtained by means of the expression (1):

$$P_{loss} = 1 - |S11|^2 - |S21|^2 \qquad (1)$$

In these cases, an important part of the incident power is neither transmitted nor absorbed; therefore it must be radiated [8]. Table 1 shows these frequencies and the corresponding value of expression (1).

Freq. (GHz)	0.75	1.66	2.22	2.40	2.63
P_{loss}	0.48	0.62	0.45	0.35	0.37

Table 1. List of frequencies with higher values of poser los.

As can be seen, these frequencies correspond to the stop-bands of the filter, except for 2.22 GHz. This one (2.22 GHz) appears due to the fact that the return losses (S11) are very low, while insertion losses have a significant value. That happens because this frequency corresponds to the resonance frequency of a CSSR's subset, as we will see below.

The following figures show the simulated RMS values of the electric (E) near-field, dB normalized to the maximum, and the radiated electric field, E_{max}, calculated by taking into account the maximum electric field components in both ϕ and θ coordinates, E_ϕ and E_θ, according to expresion (2).

$$E_{max} = \sqrt{(E_{\emptyset,max})^2 + (E_{\theta,max})^2} \qquad (2)$$

The radiation pattern has been studied at the yz plane (ϕ = 90º), which allows to visualize the radiation impact.

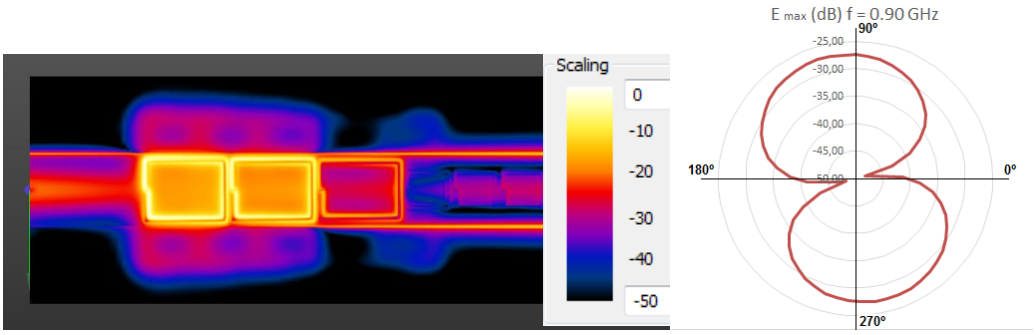

Figure 4. Simulated RMS values for E near-field and normalized radiation pattern at 0.90 GHz.

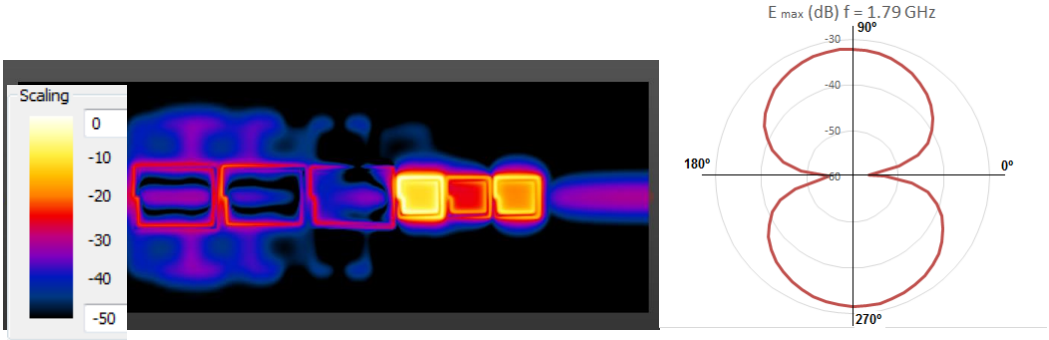

Figure 5. Simulated RMS values for E near-field and normalized radiation pattern at 1.79 GHz.

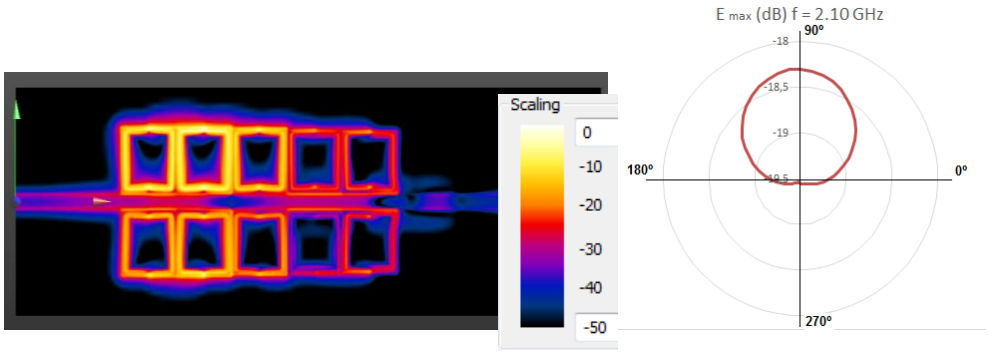

Figure 6. Simulated RMS values for E near-field and normalized radiation pattern at 2.10 GHz.

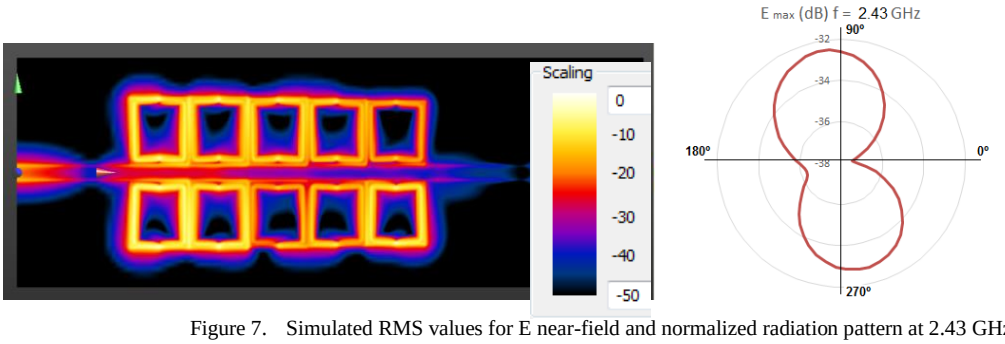

Figure 7. Simulated RMS values for E near-field and normalized radiation pattern at 2.43 GHz.

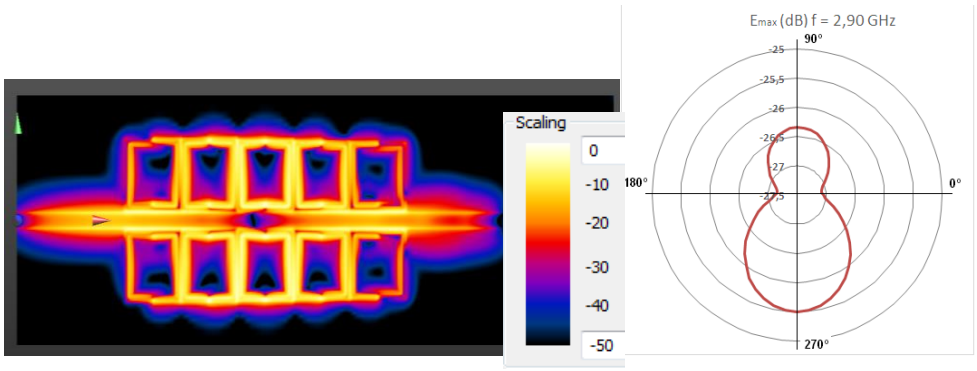

Figure 8. Simulated RMS values for E near-field and normalized radiation pattern at 2.90 GHz.

As can be seen in Figs. 4-8, the emission takes place mainly at the corresponding resonators, except for the 2.22 GHz, which corresponds to the resonance frequency of a subset of the SRRs resonators and, for this reason, the S11 parameter is very low at this frequency, while the S21 indicates that there are not significant insertion losses. In this case, the emission is directed only to z-positive (perpendicular to the top board layer) values.

It is also remarkable, that the main emissions occur at the base frequency 0.90 GHz and its harmonic: 1.79 GHz (≈ 2·0.90) and 2.90 GHz (≈ 3·0.90).

4. CONCLUSIONS

A multiband filter, designed by SRR's and CSR's, was tested and simulated. The experimental data show a good response, with rejections levels up to 20dB/40dB. The simulations of both near and far-field were done and the results are shown, further measurements shall be done to assure that the device can satisfy the conventional electromagnetic normative.

ACKNOWLEDGMENT

This work has been partially supported by Generalitat de Catalunya (SGR2009-1425) and the Spanish Government (TEC2010-18550).

REFERENCES

[1].S. Shahparnia and O.M. Ramahi, "Electromagnetic interference (EMI) reduction drom printed circuit boards (PCB) using electromagnetic bandgap structures", IEEE Transactions on Electromagnetic Compatibility, vol. 46, pp. 292-303, November 2004.
[2].B.M. Iravani and O.M. Ramahi, "Design, implementation and testing of miniaturized electromagnetic bandgap structures for broadband switching noise mitigation in high-speed PCBs", IEEE Transactions on Advanced Packaging, vol. 30, pp. 171-179, May 2007.
[3].J.B. Pendry, A.J. Holden, D.J. Robbins and W.J. Stewart, "Magnetism from conductors and enhanced nonlinear phenomena", IEEE Trans. Microwave Theory and Techniques, vol. 47, pp. 2075-2084, November 1999.
[4].J.D. Baena, J. Bonache, F. Martin, R. Marqués, F. Falcone, T. Lopetegui, M.A.G. Laso, J. García-García, I. Gil, M. Flores Portillo and M. Sorolla. "Equivalent-circuit models for SRRs and CSRRs coupled to planar transmision lines". IEEE Transactions on Microwave Theory and Techniques, vol. 53, pp. 1451-1461, April 2005.
[5].D. Pérez, I. Gil, J. Gago, R. Fernández-García, J. Balcells, S. Member, D. González, N. Berbel, and J. Mon, "Reduction of Electromagnetic Interference Susceptibility in Small-Signal Analog Circuits Using Complementary Split-Ring Resonators,", IEEE Trans. On Comp., Pack. And Manuf. Tech., Vol. 2, no. 2, pp. 240–247, October 2012.
[6]."SEMCAD." Schmid & Partner Engineering AG (SPEAG).
[7].I. Gil, R. Fernández, J. Gago, and J. Balcells, "Multiband EMI filter based on metamaterials," IEICE Electron. Express, vol. 7, no. 9, pp. 563–568, May 2010.
[8] Mohammed M. Bait-Suwailam and Omar M. Ramahi. "Ultrawideband Mitigation of Simultaneous Switching Noise and EMI Reduction in High-Speed PCBs Using CSRR". IEEE Transactions on Electromagnetic Compatibility, Vol. 54, No. 2, April 2012.